

High-Lift Devices for a Delta Wing Installed Around a Trailing-Edge

Koji Miyaji* and Tomoyuki Arasawa†
Yokohama National University, Yokohama 240-8501, Japan

Three devices to improve the aerodynamic characteristics of a delta wing at low speeds and high angles of attack are computationally examined. These are two types of blowing at the trailing edge and a slotted flap. All three are commonly employed on rectangle wings. They all show favorable effects, namely, chordwise blowing increases the lift considerably. The effectiveness in strengthening the leading-edge vortex is higher for chordwise blowing than lateral blowing. It is observed that, although the jet slots are installed at a trailing edge, the blowing strengthens the leading-edge separation vortex over the delta wing. This motivated an investigation of the use of a slotted flap. The flap also increases the lift of the wing, as well as the total lift due to both the wing and the flap, but the effect on the leading-edge vortices is smaller than both types of blowing.

Nomenclature

C_D	= drag coefficient
C_L	= lift coefficient
C_P	= pressure coefficient
C_μ	= nondimensional momentum of jet
L	= total length of the fuselage of wind-tunnel model
q_∞	= freestream-dynamic pressure
S_{wing}	= surface area of wing
V	= velocity magnitude
α	= angles of attack
ρ	= density

Subscript

j	= properties at jet exit
-----	--------------------------

Introduction

AIRCRAFT with delta wings are usually designed to achieve good aerodynamic performance in the transonic or supersonic flight regimes. At low speeds and high angles of attack, the performance of these aircraft is not favorable, and consequently, a long distance is necessary for takeoff and landing. The flow over a delta wing for such conditions is mainly governed by a pair of leading-edge separation vortices. Various types of blowing, or jets, have been proposed in previous studies (for example, in Refs. 1–5) aimed at strengthening or maintaining the vortices. In Ref. 4, Miyaji et al. numerically clarified the mechanism of trailing-edge lateral blowing on a configuration whose good performance had been experimentally verified.⁵ The benefits of blowing were increase in lift at all angles of attack, improvement of the lift-to-drag ratio, and recovery of the leading-edge vortices at high angles of attack near stall conditions. The favorable effects of blowing at high angles of attack motivated the present work. The objectives of the present paper are to examine new blowing strategies through the use of numerical simulations and to compare their effectiveness with previous work. Furthermore, the performance of a slotted flap is examined because

the gap between the wing and the flap is expected to play an important role. Our final objective is to determine whether it is practical to use blowing or the slotted flap for short-distance takeoff and landing on a delta wing configuration.

Flow Configuration

The previous trailing-edge lateral blowing, and the new blowing scheme are schematically shown in Figs. 1a and 1b. In Fig. 1a, the jet is injected under the trailing edge in the lateral (outboard) direction, whereas in Fig. 1b the jet is injected in the chordwise direction from a slit opening at the trailing edge. This is similar to a jet flap or augmentor wing that were originally proposed for rectangular wings. The new blowing scheme is termed trailing-edge chordwise blowing. The slotted flap, which has a gap between the wing and the flap, is shown in Fig. 1c. This is also usually used for rectangular wings.

The wing-body configuration shown in Fig. 2 is studied. This simplified supersonic transport configuration with double delta wings is the same as the wind-tunnel model examined in Ref. 6. The leading-edge sweep angle of the inner and the outer wing are 72.7 and 52.2 deg, respectively. The airfoil in the spanwise cross section is a 6% circular arc. The experiments were conducted to study the effect of the trailing-edge lateral blowing.

The flow conditions are as follows. The freestream Mach number is 0.3, and the Reynolds number is 1×10^6 . The angles of attack are 0, 10, 20, 30, and 35 deg. A sonic jet is specified at the jet slot for both types of blowing. The stagnation pressure of the jet is 9.8×10^5 N/m², which is the same as in the experiment. The stagnation pressure determines the nondimensional momentum of the jet C_μ given by the following formula:

$$C_\mu = \frac{\int \int_{A_j} \rho_j V_j \cdot dA_j}{q_\infty S_{\text{wing}}}$$

Numerical Methods

The three-dimensional thin-layer Navier–Stokes equations are numerically solved by a finite difference method. The inviscid fluxes are calculated by Roe's flux difference splitting, and the MUSCL interpolation is used to achieve spatially third-order accuracy. The viscous terms are calculated by second-order central differencing. The time-integration algorithm is a lower-upper alternating direction implicit factorization method⁷ and the local time step is used. The standard Baldwin–Lomax turbulence model is used for the slotted flap configuration to avoid numerical flow separation. The eddy viscosity is computed only near the body surface because including the leading-edge separation vortices results in excessive eddy viscosity.

Received 21 May 2001; revision received 13 January 2003; accepted for publication 30 January 2003. Copyright © 2003 by Koji Miyaji and Tomoyuki Arasawa. Published by the American Institute of Aeronautics and Astronautics, Inc., with permission. Copies of this paper may be made for personal or internal use, on condition that the copier pay the \$10.00 per-copy fee to the Copyright Clearance Center, Inc., 222 Rosewood Drive, Danvers, MA 01923; include the code 0021-8669/03 \$10.00 in correspondence with the CCC.

*Lecturer, Department of Ocean and Space System Engineering, 79-5 Tokiwadai, Hodogaya-ku. Member AIAA.

†Graduate Student, Department of System Design, 79-5 Tokiwadai, Hodogaya-ku.

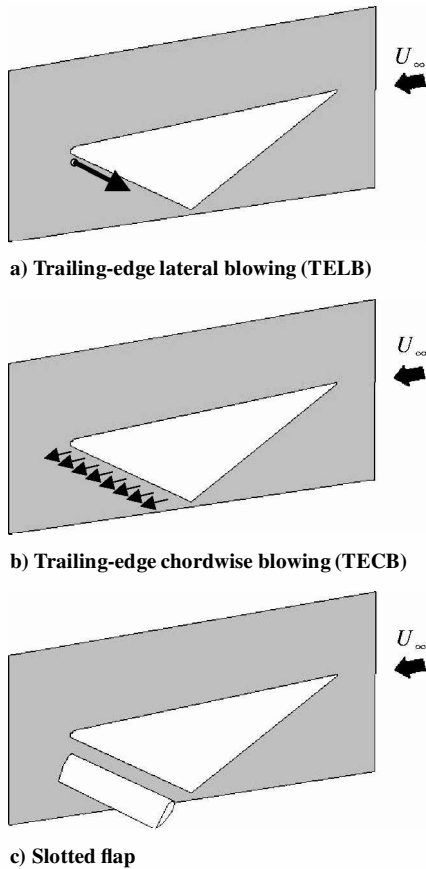


Fig. 1 Schematic of high-lift devices.

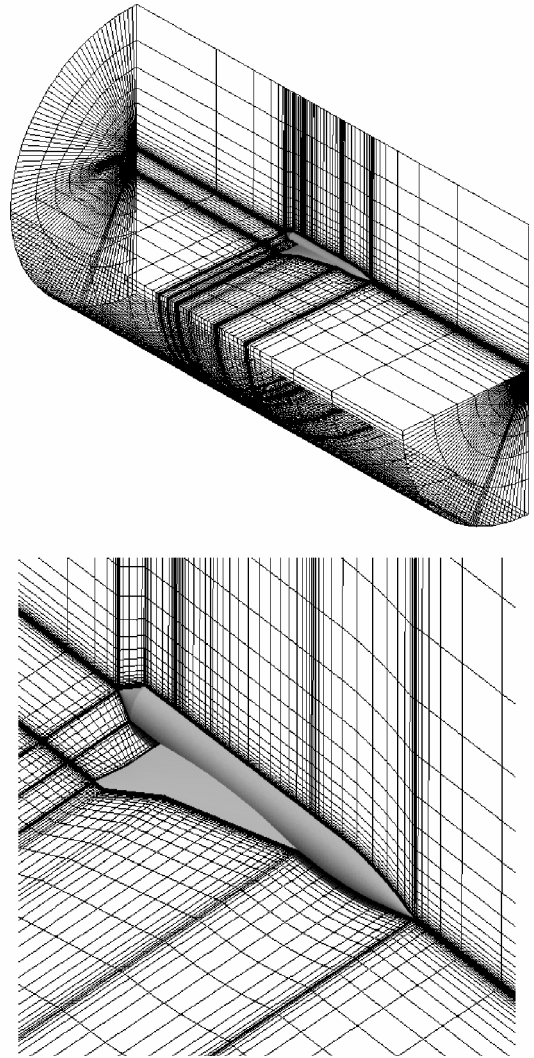


Fig. 3 Computational grids.

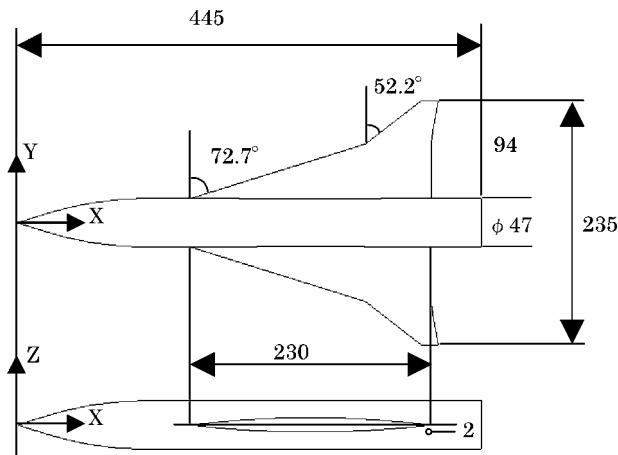


Fig. 2 Model configuration, dimensions in millimeters.

Figure 3 shows an algebraically generated H-O grid that is typical of that used for all of the simulations. The grid dimensions are $91 \times 91 \times 41$ points, resulting in about 340,000 grid points in total. Overset grid methods⁸ are used. In the blowing simulation, the overset grids are used to increase the local grid resolution around the jet,⁴ whereas in the simulation of a slotted flap, they are used to avoid the difficulty of generating a single computational grid around a wing and a flap.

Results and Discussions

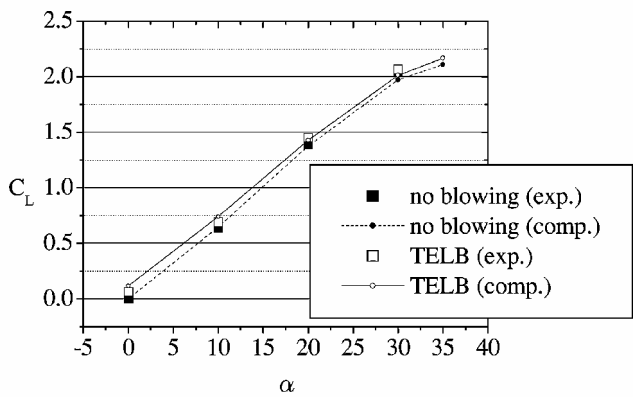
Numerical accuracy was first examined by comparing the available experimental data with the simulation. Then the effects of the flow control devices were studied in the simulations by comparing the different numerical results.

Trailing-Edge Lateral Blowing

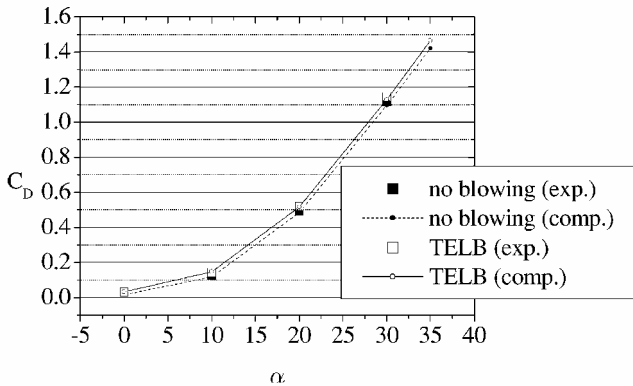
The results for the lateral blowing are shown first. As shown in Fig. 2, the diameter of the jet slot is 2 mm, and the center of the slot is 2 mm below the trailing edge, the length of which is about 1% of the root chord length. A fine overset grid, of dimensions $25 \times 41 \times 27$ is used around the slot. Figures 4a and 4b show the effect of the blowing on the aerodynamic forces. The experimental and numerical results compare well for nonblowing cases, thus, verifying the accuracy of the simulation. The grid resolution around the jet exit is not sufficient to resolve the turbulent boundary layer inside the jet slot; thus, a laminar velocity profile is specified as the boundary condition. However, with this boundary condition, the integrated momentum of the jet

$$\int \int_{A_j} \rho_j V_j V_j \cdot dA_j$$

is smaller than the actual value; thus, a one-and-one-half times larger diameter is used in the computation to specify properly the jet momentum. Then the value of C_{μ} is 0.045. The results in Figs. 4a and 4b show the blowing effects and confirm the suitability of the described jet condition. The drag, as well as the lift, is increased at all angles of attack. The reason for the change of the aerodynamic forces and the features of the blowing can be seen in the surface pressure distributions in Figs. 5b–5d. The pressure coefficients at the three chordwise stations at 30-deg angle of attack are shown (Fig. 5a). As observed previously,⁴ the pressure increases on the lower surface of the wing and decreases on the upper surface. These



a) Lift



b) Drag

Fig. 4 Lift and drag distribution with and without TELB.

changes are apparent up to the leading edge (Fig. 5a), although the blowing is applied beneath the trailing edge. This large change is due to the blockage effect ahead of the jet core on the lower surface and due to the acceleration effect just below the trailing edge, namely, between the jet core and the main flow. These result in a pressure decrease. The low pressure near the trailing edge also accelerates the upper surface flow. Figures 6a and 6b show the streamlines from the apex of the wing and the reverse flow (negative velocity in X direction) region over the wing. The reverse flow completely disappears with the blowing. Although the lift increase is not as large, the more uniform vortical flow is apparently favorable from the viewpoint of aircraft stability. However what is important for short takingoff and landing is an absolute value of the lift.

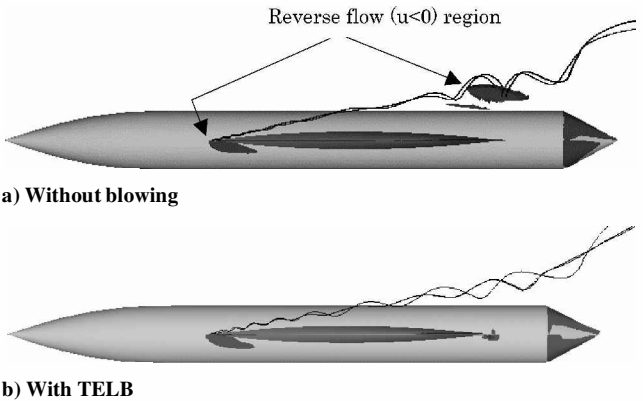
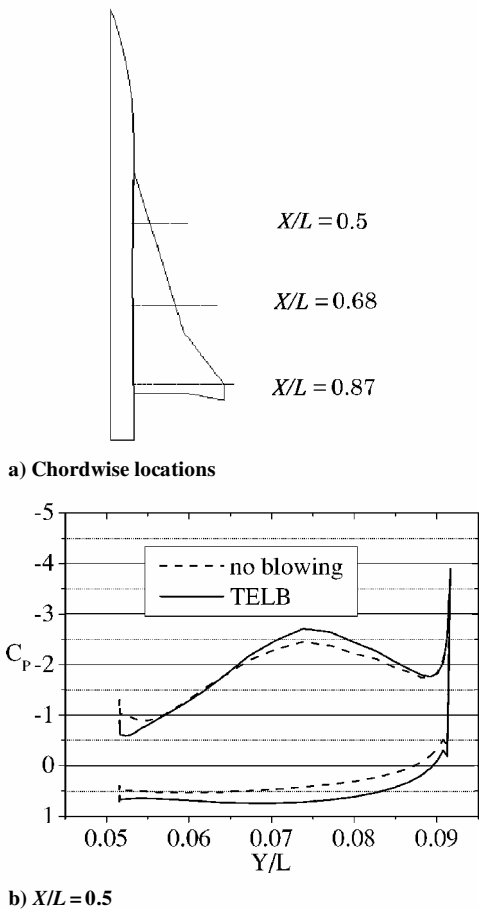
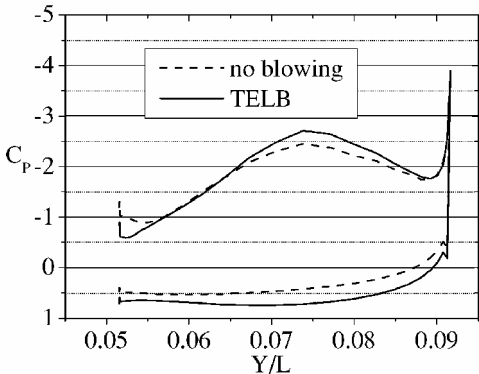


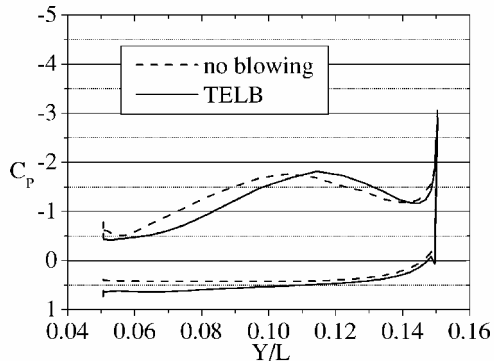
Fig. 6 Streamlines and reverse flow region, $\alpha = 35$ deg.



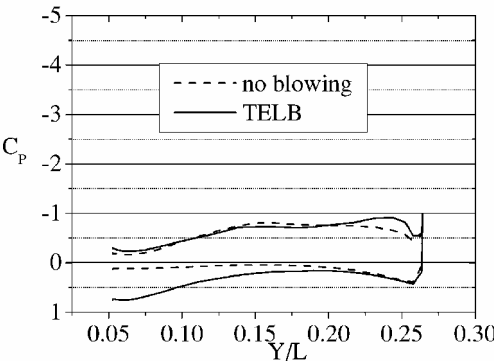
a) Chordwise locations



b) $X/L = 0.5$

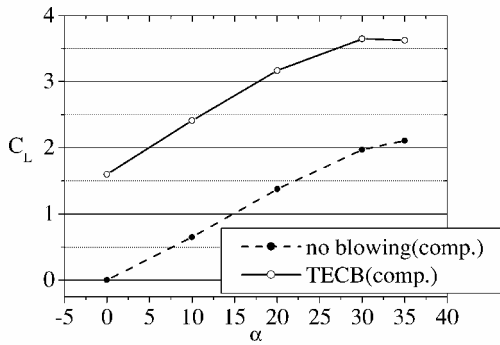


c) $X/L = 0.68$

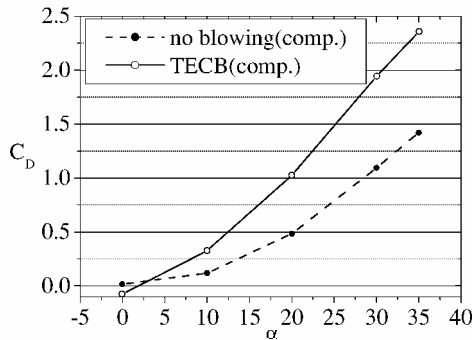


d) $X/L = 0.87$

Fig. 5 Spanwise pressure distribution with and without TELB, $\alpha = 30$ deg.



a) Lift



b) Drag

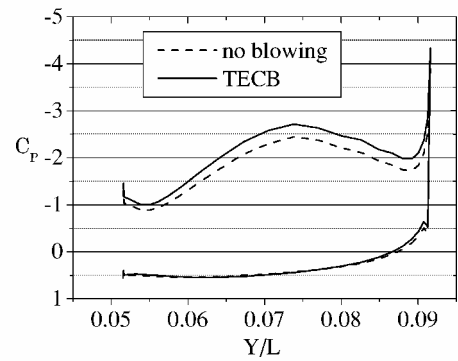
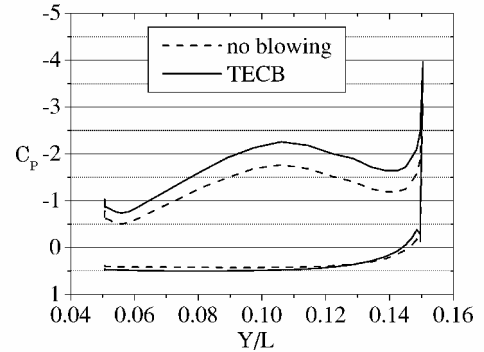
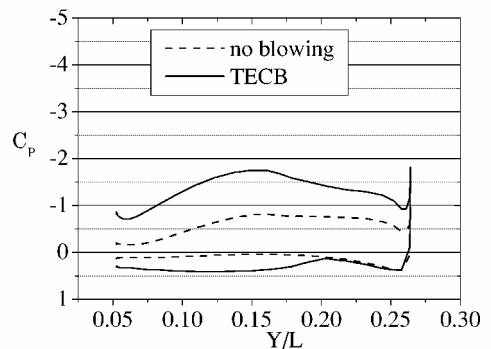
Fig. 7 Lift and drag distribution with and without TECB.

Trailing-Edge Chordwise Blowing

The beneficial effects of lateral blowing motivated the study of a blowing approach, namely, chordwise blowing. As already discussed, the effect of lateral blowing is to prevent flow reversal around the trailing edge, which disturbs the smooth flow over the wing. A similar effect is expected from the trailing-edge chordwise blowing, which is schematically shown in Fig. 1b. The jet boundary condition is prescribed along the trailing edge with the velocity directed in the X direction (Fig. 2). Although the stagnation pressure of the jet is the same as in the lateral blowing case, the value of C_{μ} becomes 0.127 because the jet exit areas are much larger than the lateral blowing case.

Figures 7a and 7b show the effect of chordwise blowing on aerodynamic coefficients, and Figs. 8a–8c show the effect on the pressure distributions. The lift is considerably increased at all angles of attack, and the increments are much larger than the lateral blowing case. It is difficult to compare the two types of blowing because the total momentum of the jet is quite different. In this paper, the ratio of the lift increase to the momentum of the jet, $\Delta C_L / C_{\mu}$, is used as a measure of the efficiency. The C_{μ} can be interpreted as the increase in the lift coefficient when the jet is directly injected downward. The values of $\Delta C_L / C_{\mu}$ are larger than unity for both types of blowing, as is shown in Fig. 9. This confirms the high efficiency of the present blowing.

The drag increases over the range of angle of attack except for the 0-deg angle-of-attack case in which the thrust of the jet works directly to reduce the drag. The drag increases are, however, smaller than the lift increments, and thus, the lift-to-drag ratios improve. With blowing, the aerodynamic forces acting in the normal direction of the wing surface (Z direction in Fig. 2) get considerably larger. The reason can be seen in Figs. 8. The decrease of pressure on the upper surface is larger with chordwise blowing than the lateral blowing at every chordwise station. In addition, an almost flat pressure distribution near the trailing edge for the nonblowing case is substantially changed. With chordwise blowing, the negative pressure coefficient peak due to the leading-edge separation vortices is recovered at the most downstream station in Fig. 8c. On the other hand, the pressure increase on the lower surface nearer to the leading edge (Figs. 8a and 8b) is barely seen. This is because chordwise blowing does not have the same blocking effect as lateral blowing.

a) $X/L = 0.5$ b) $X/L = 0.68$ c) $X/L = 0.87$ Fig. 8 Spanwise pressure distribution with and without TECB, $\alpha = 30$ deg.

Although reversed flow region is not eliminated with chordwise blowing, it is observed that the flow reversal is moved downstream and the smooth flow is maintained over the wing. In the preliminary computation for a simple delta wing alone, the chordwise blowing also diminished the reverse flow, and it is thought that the vortex breakdown is sensitive to the pressure changes due to the existence of the fuselage.

Slotted Flap

The computed results of the two types of blowing suggest that a slotted flap, which is commonly used for rectangular wings, will have an effect similar to blowing. This concept has been examined in Ref. 9, but in that work the effects at high angle of attack were not studied in detail. The presence of the slotted flap causes a pressure increase on the lower surface of the delta wing. The high-momentum flow from the gap between the wing and the flap induces the upper flow to move downstream more smoothly. This is expected to strengthen the leading-edge vortex. An overset grid method that treats the wing and the flap simultaneously is required for the computation. The configuration of the flap is a simple rectangular wing, the cross section of which is a NACA0012 airfoil. Various locations of the flap were examined, and the results for the location shown in Fig. 10 are presented here.

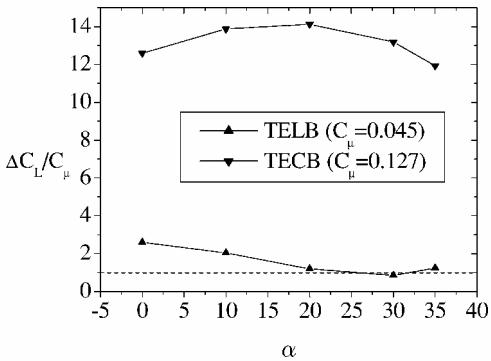


Fig. 9 Ratio of lift increase ΔC_L to momentum of the jet C_μ .

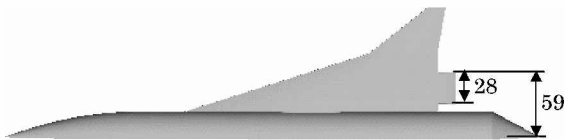


Fig. 10 Slotted flap locations.

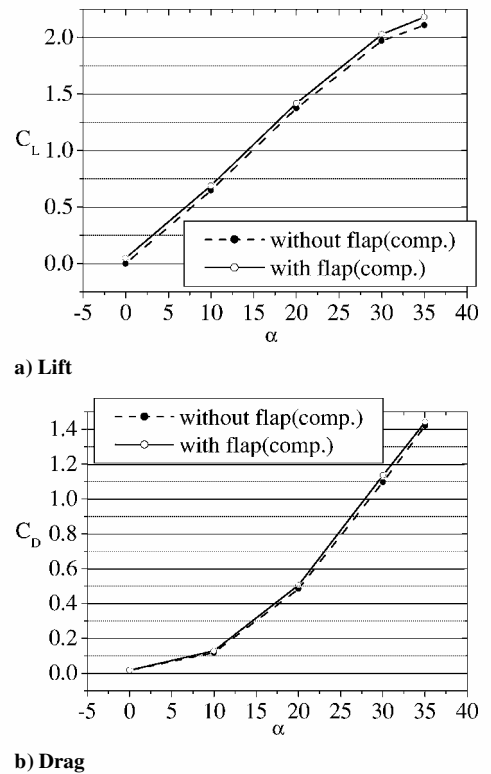


Fig. 11 Lift and drag distributions with and without slotted flap.

Figures 11a and 11b show aerodynamic coefficients for the slotted flap case. The increments of lift and drag are similar to the trailing-edge lateral blowing case shown in Figs. 4. However, the pressure distributions shown in Figs. 12a–12c are rather different from the lateral and the chordwise blowing case. In Fig. 12c, the pressures increased on the lower surface and decreased on the upper surface as expected, but these changes are limited to the trailing edge. This result suggests that the slotted flap works to increase the lift at moderate angles of attack, but it is not effective in strengthening the leading-edge vortices at high angles of attack. It is thought that this is because the flow acceleration between the wing and the flap is not as substantial as compared with the blowing cases. A simple airfoil is used in the present study, and it is thought that careful design of the flap may increase the performance of the flap. However, the present results show blowing to have better effectiveness.

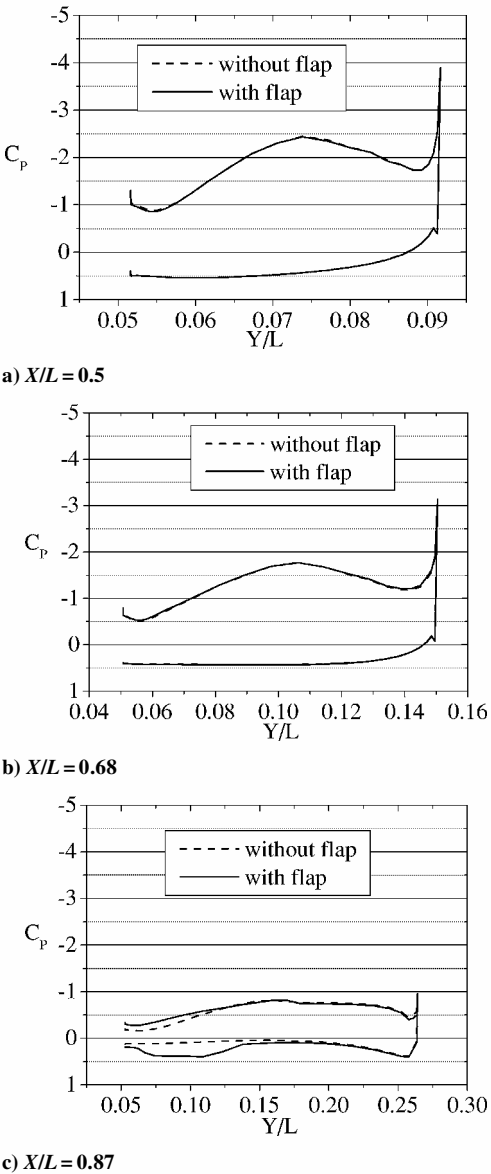


Fig. 12 Spanwise pressure distribution with and without slotted flap, $\alpha = 30$ deg.

Summary

The performance of three types of high-lift devices, trailing-edge lateral blowing, trailing-edge chordwise blowing, and a slotted flap, are examined. Simulations clarify the mechanism of the change in the aerodynamic forces and in the flow features of each device. The lift is increased at all angles of attack, and the lift-to-drag ratios are improved. In addition, both types of blowing strengthen the leading-edge vortices at high angles of attack. Two factors are observed to delay the vortex breakdown. The first is that the flow is prevented from turning from the lower to upper surface of the wing at the trailing edge. The second is flow is induced downstream by the jet stream. Trailing-edge lateral blowing causes pressure changes on both the upper and the lower surface of the wing: These changes act to increase the lift. Trailing-edge chordwise blowing mainly affects the flow on the upper surface, but the pressure decrease is larger compared with that of lateral blowing. The resulting increase in lift is much larger. Although the slotted flap is also effective in increasing the lift at moderate angles of attack, it is not effective in strengthening the leading-edge vortices.

References

¹Bradley, R. D., and Wray, W. O., "A Conceptual Study of Leading-Edge Vortex Enhancement by Blowing," *Journal of Aircraft*, Vol. 11, No. 1, 1974, pp. 33–48.

²Yea, D. T., Tavella, D. A., Roberts, L., and Fujii, K., "Navier–Stokes Computation of the Flowfield over Delta Wings with Spanwise Leading Edge Blowing," AIAA Paper 88-2558, June 1988.

³Yeh, D. T., Tavella, D. A., Roberts, L., and Fujii, K., "Numerical Study of the Effect of Tangential Leading Edge Blowing on Delta Wing Vortical Flow," AIAA Paper 89-0341, Jan. 1989.

⁴Miyaji, K., Fujii, K., and Karashima, K., "Enhancement of the Leading-Edge Separation Vortices by Trailing-Edge Lateral Blowing," *AIAA Journal*, Vol. 34, No. 9, 1996, pp. 1943–1945.

⁵Karashima, K., and Sato, K., "The Effect of Lateral Blowing on Aerodynamic Characteristics of Low Aspect Ratio Wings," *Journal of the Japan Society for Aeronautical and Space Sciences*, Vol. 37, No. 425, 1983, pp. 14–20 (in Japanese).

⁶Kamishita, K., Aso, S., Karashima, K., and Sato, K., "A Study on Aerodynamic Characteristics Improvement of Next-Generation SST Wing by Lateral Blowing," *Proceeding of Japanese Fluid Dynamics Conference*, The Japan Society for Aeronautical and Space Sciences, 1999, pp. 349–352 (in Japanese).

⁷Obayashi, S., Matsushima, K., Fujii, K., and Kuwahara, K., "Improvement in Efficiency and Reliability for Navier–Stokes Computations Using the LU-ADI Factorization Algorithms," AIAA Paper 86-0338, Jan. 1986.

⁸Fujii, K., "Unified Zonal Method Based on the Fortified Solution Algorithm," *Journal of Computational Physics*, Vol. 118, No. 1, 1995, pp. 92–108.

⁹Paulson, J. W., Jr., Quinto, P. F., and Banks, D. W., "Investigation of Trailing-Edge-Flap Spanwise-Blowing Concepts on an Advanced Fighter Configuration," NASA TP 2250, Jan. 1984.